Electron redistribution induced by p–d orbital hybridization in Co_2P/FeP nanosheets boosts water electrooxidation†

Qiyan Sun[a], Yu Miao[a], Ruixue Zhang[a], Guang-Rui Xu[a,*], Chuanfang Zhang[c], Kang Liu[b], Zexing Wu[b], and Lei Wang[a,b,*]

[a] Key Laboratory of Eco-chemical Engineering, Key Laboratory of Optic-electric Sensing and Analytical Chemistry of Life Science, Taishan Scholar Advantage and Characteristic Discipline Team of Eco Chemical Process and Technology, School of Materials Science and Engineering, Qingdao University of Science and Technology, Qingdao 266042, PR China

[b] College of Chemistry and Molecular Engineering, Qingdao University of Science and Technology, Qingdao 266042, PR China

[c] Shandong Weima Equipment Science & Technology Co., Ltd., Dongying, 257000, China

E-mail: xugrui@gmail.com (G.-R. Xu); inorchemwl@126.com (L. Wang)

Computational Details

All DFT calculations were performed using the Vienna ab initio simulation package (VASP5.4.4).[1] The exchange-correlation is simulated with PBE functional and the ion-electron interactions were described by the PAW method.[2,3] The vdWs interaction was included by using empirical DFT-D3 method.[4] The Monkhorst-Pack-grid-mesh-based Brillouin zone k-points are set as 2×2×1 for all periodic structure with the cutoff energy of 400 eV. The convergence criteria are set as 0.02 eV A^{-1} and 10^{-5} eV in force and energy, respectively.

The free energy calculation of species adsorption (ΔG) is based on Nørskov *et al*'s hydrogen electrode model.[5]

$$\Delta G = \Delta E + \Delta E_{ZPE} - T\Delta S + eG_U \quad (1)$$

Herein ΔE, ΔE_{ZPE}, and ΔS respectively represent the changes of electronic energy, zero-point energy, and entropy that caused by adsorption of intermediate, while the eG_U is free energy change contributed by the applied potential, 1.23 V in typical OER. The entropy of $H^+ + e^-$ pair is approximately regarded as half of H_2 entropy in standard condition.[6]

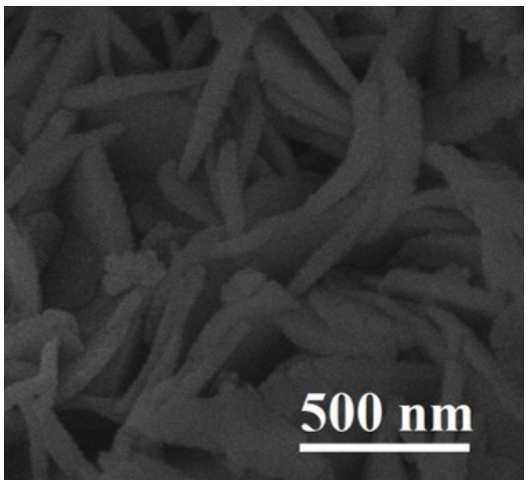

Fig. S1 SEM image of FeP nanosheets.

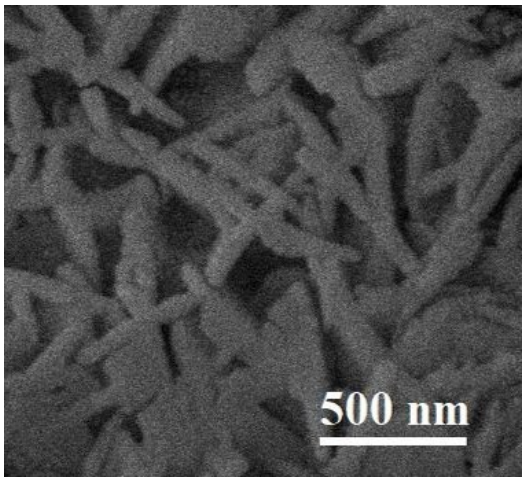

Fig. S2 SEM image of Co_2P nanosheets.

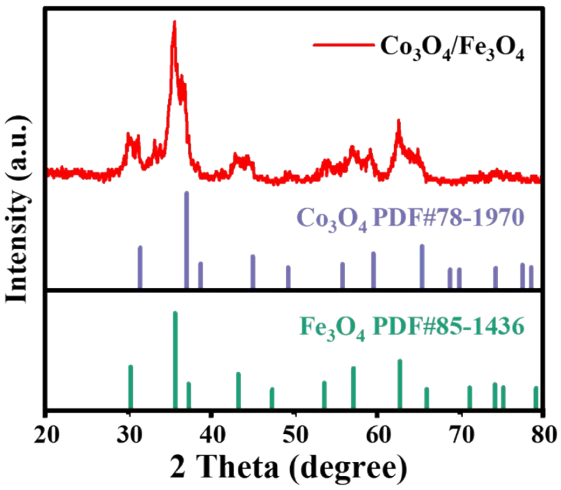

Fig. S3 XRD patterns of the Co_3O_4/Fe_3O_4 nanosheets.

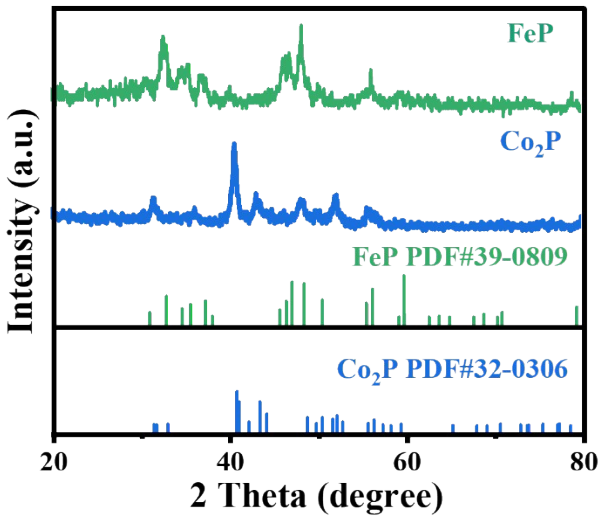

Fig. S4 XRD patterns of the FeP and Co_2P nanosheets.

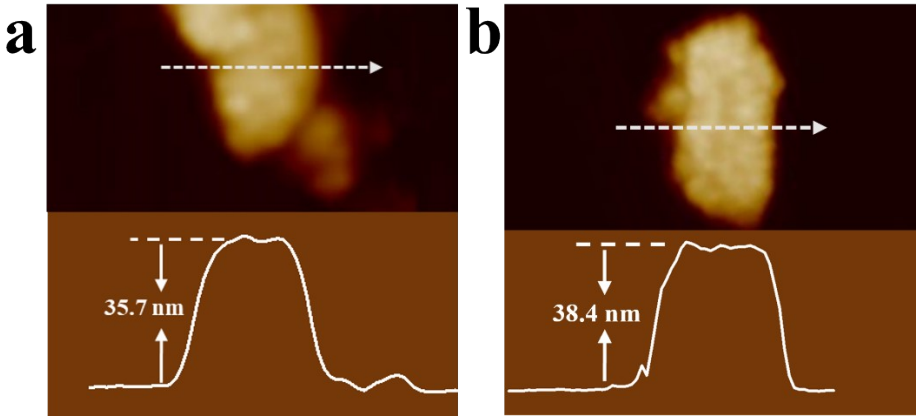

Fig. S5 Co_2P/FeP nanosheets of AFM image.

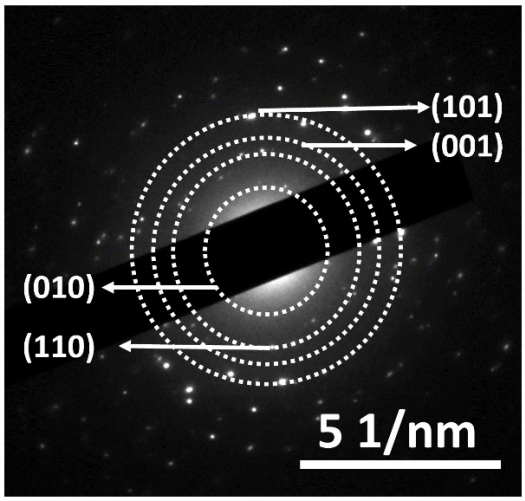

Fig. S6 Co_2P/FeP nanosheets of experimental SAED pattern.

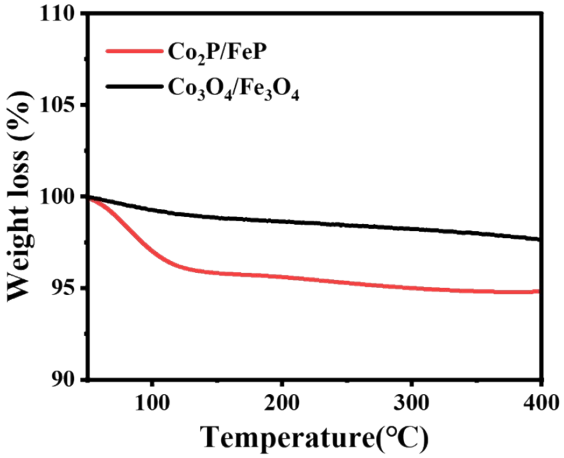

Fig. S7 TGA curves of Co_2P/FeP nanosheets and their derived Co_3O_4/Fe_3O_4 nanosheets.

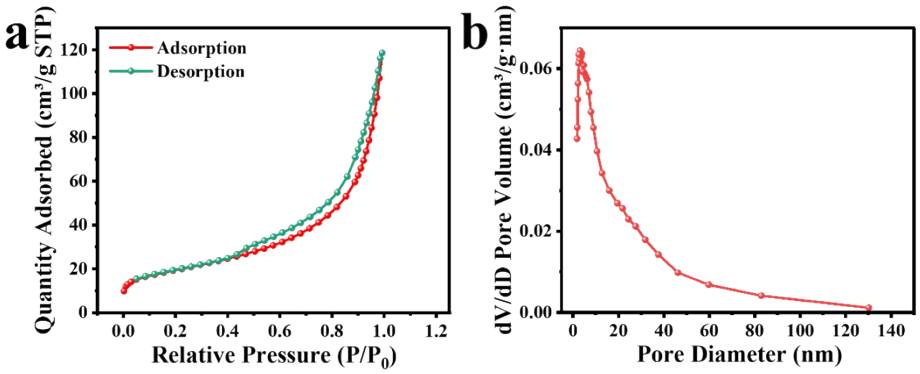

Fig. S8 (a) Nitrogen adsorption-desorption isotherm, and (b) pore size distribution for Co_2P/FeP nanosheets.

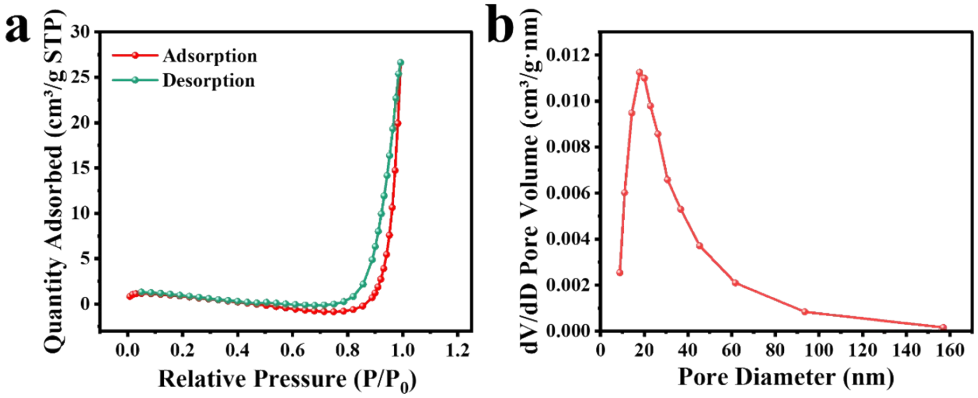

Fig. S9 (a) nitrogen adsorption-desorption isotherm, and (b) pore size distribution for Co_3O_4/Fe_3O_4 nanosheets.

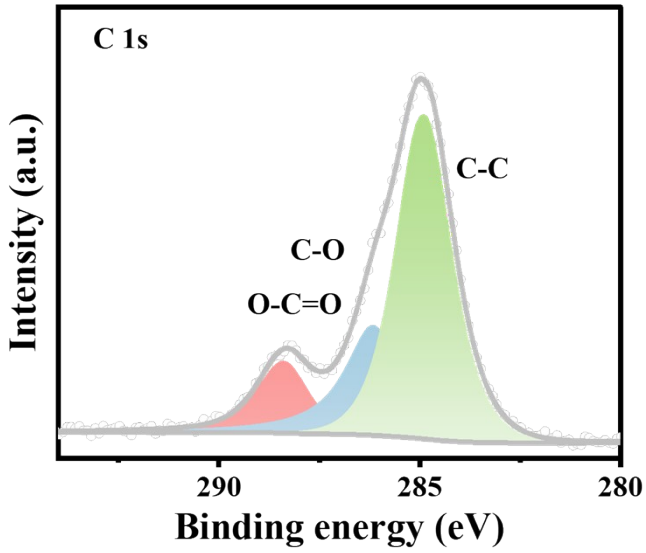

Fig. S10 C 1s XPS spectrum of Co_2P/FeP nanosheets.

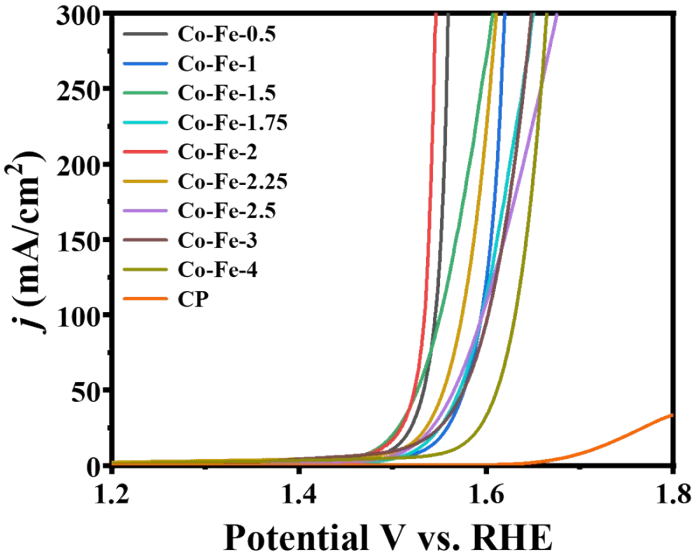

Fig. S11 LSV curves of a series of Co_2P/FeP nanosheets with different Co/Fe ratios measured in 1 M KOH.

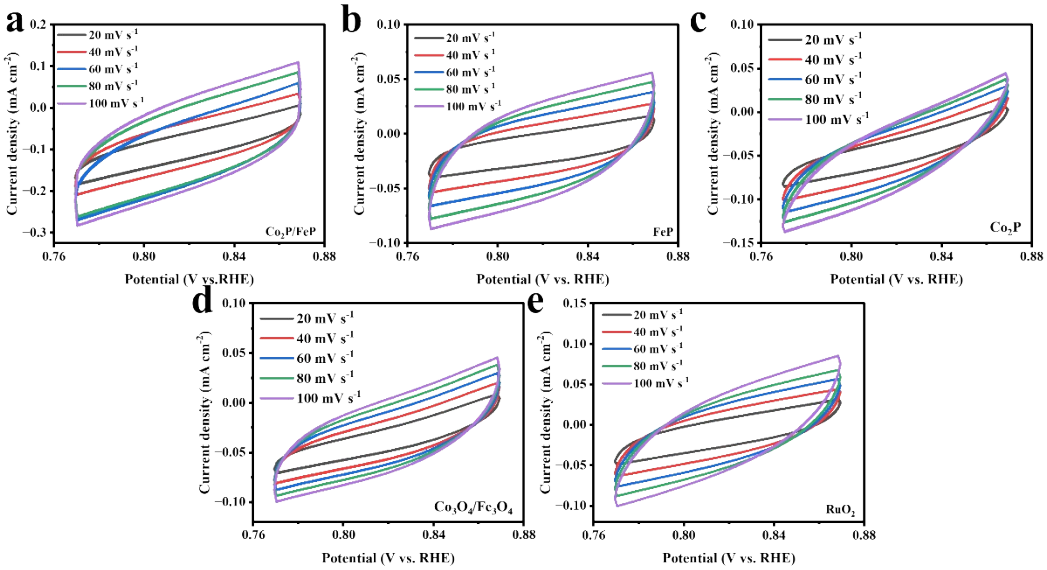

Fig. S12 CV curves at different scan rates (20-100 mV s^{-1} with the interval of 20 mV s^{-1}) of (a) Co_2P/FeP nanosheets. (b) FeP nanosheets. (c) Co_2P nanosheets. (d) Co_3O_4/Fe_3O_4 nanosheets and (e) commercial RuO_2 catalysts during OER process under 1 M KOH solution.

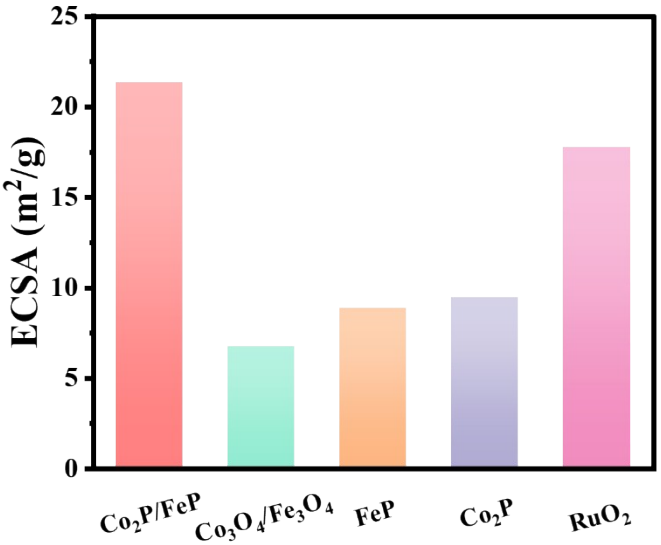

Fig. S13 ECSA of (a) Co_2P/FeP nanosheets, (b) FeP nanosheets, (c) Co_2P nanosheets, (d) Co_3O_4/Fe_3O_4 nanosheets, and (e) commercial RuO_2 catalysts during OER process under 1 M KOH solution.

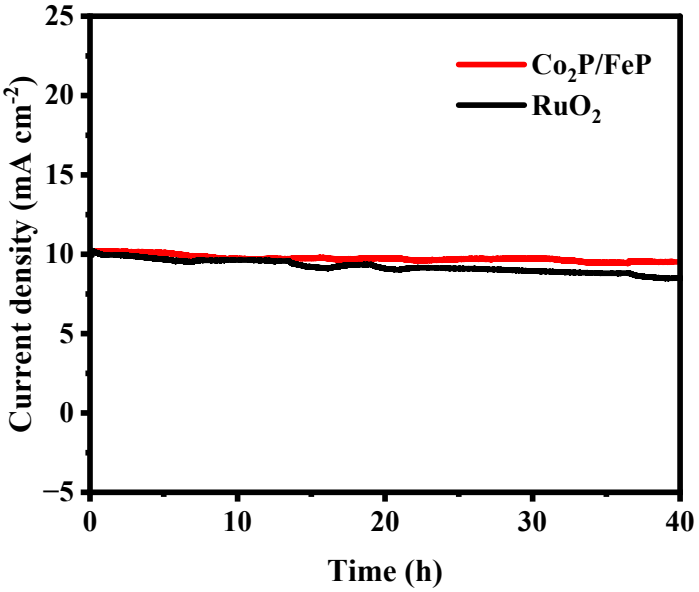

Fig. S14 The long-term durability test of Co_2P/FeP nanosheets and commercial RuO_2 at 10 mA cm^{-2} in 1 M KOH solution.

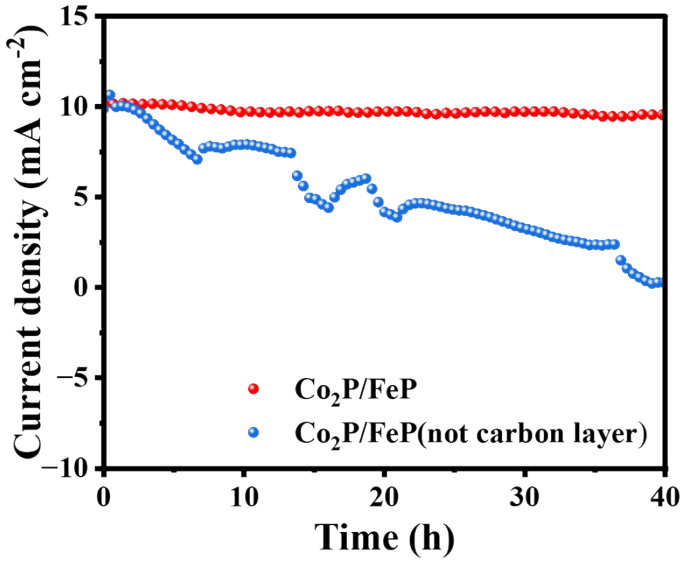

Fig. S15 Chronoamperometric curve for Co_2P/FeP nanosheets and Co_2P/FeP without carbon layer.

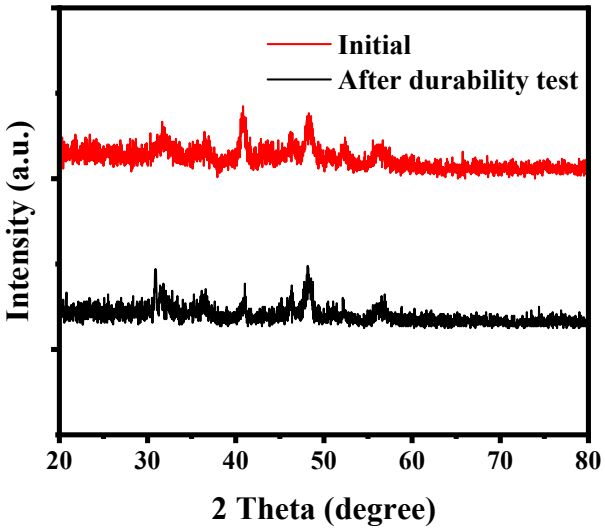

Fig. S16 XRD patterns of the Co_2P/FeP nanosheets after the long-term durability test.

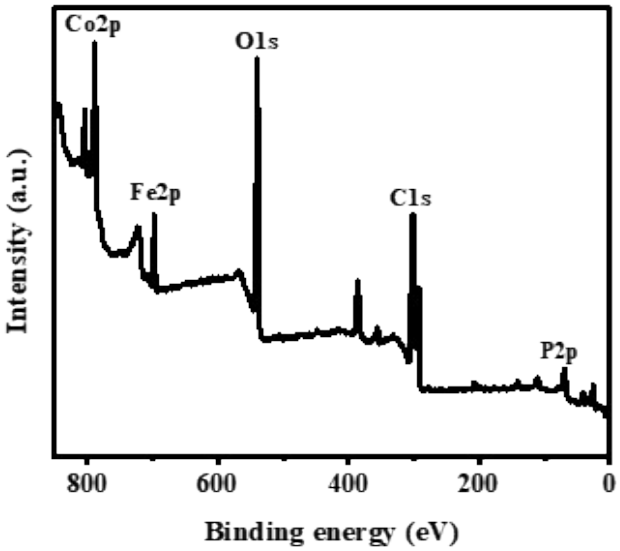

Fig. S17 The full XPS spectrum of Co_2P/FeP nanosheets after the long-term durability test.

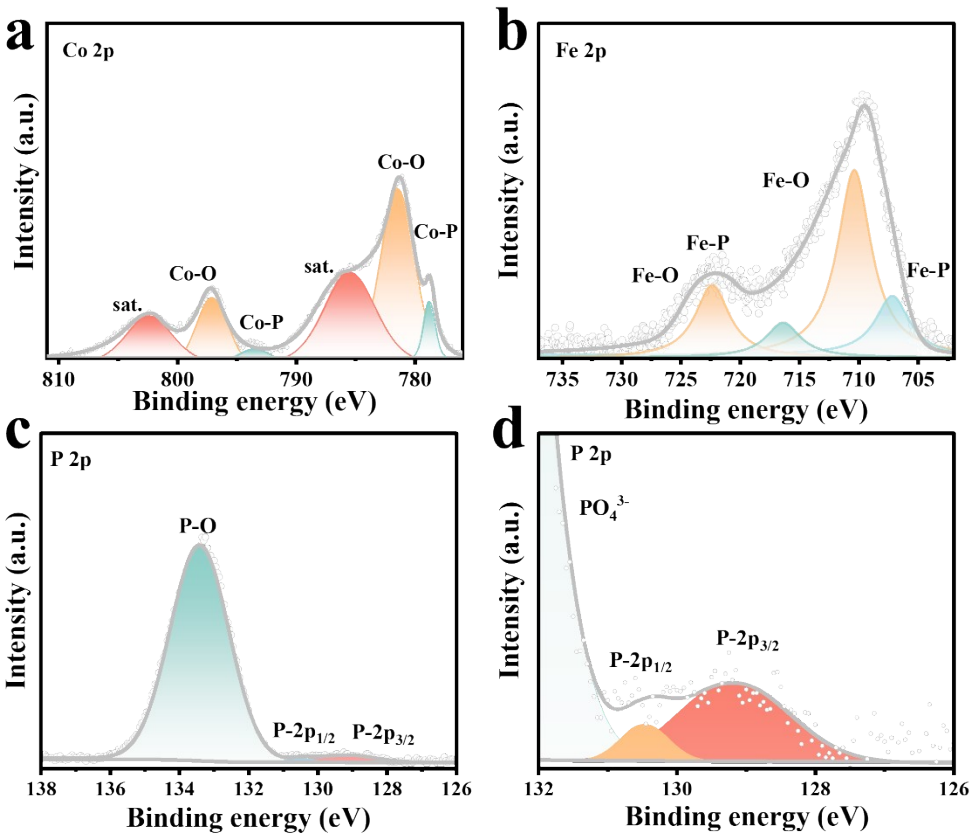

Fig. S18 XPS spectra of (a) Fe 2p, (b) Co 2p, and (c, d) P 2p for Co_2P/FeP nanosheets after the long-term durability test.

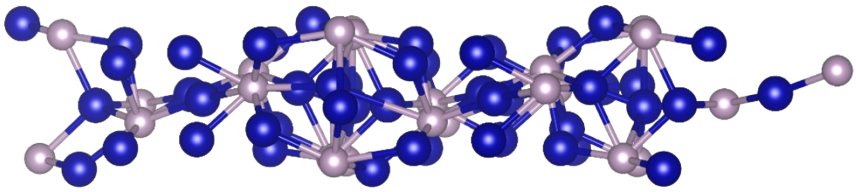

Fig. S19 Structure model of Co_2P nanosheets.

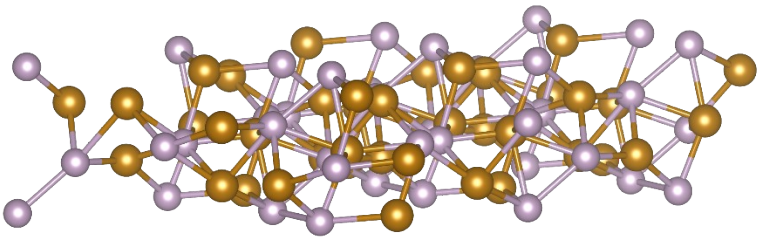

Fig. S20 Structure model of FeP nanosheets.

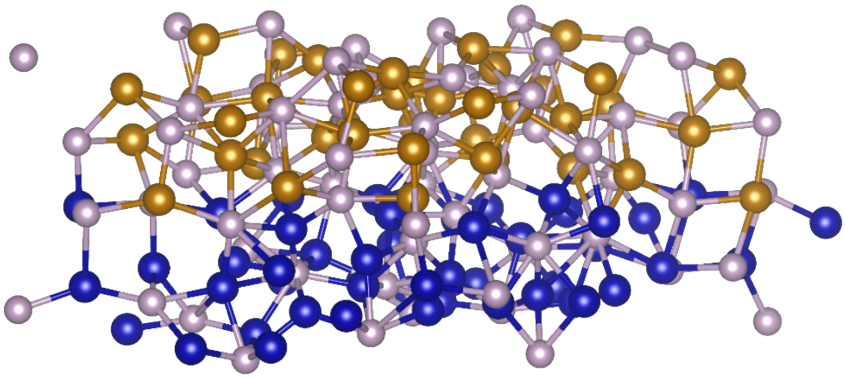

Fig. S21 Structure model of Co_2P/FeP nanosheets.

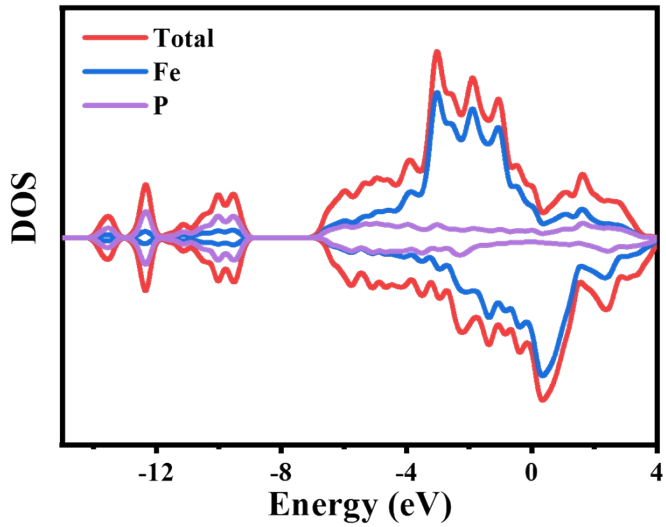

Fig. S22 Calculated DOS profiles of FeP nanosheets.

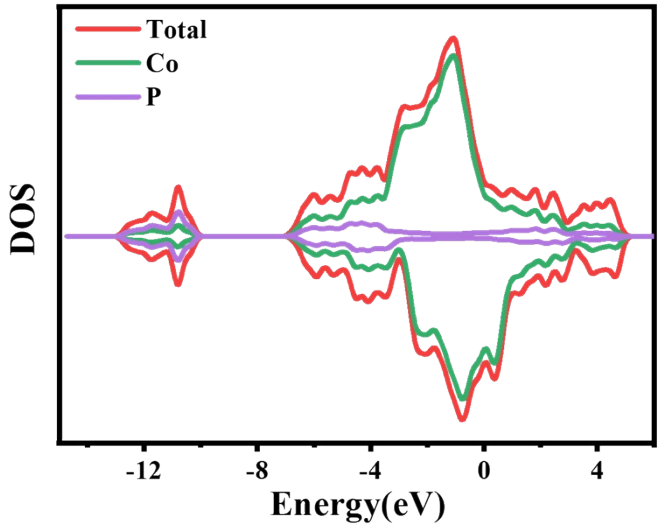

Fig. S23 Calculated DOS profiles of Co_2P nanosheets.

Table S1 A series of Co_2P/FeP nanosheets with varying Co/Fe synthetic parameter ratios and their corresponding properties.

Entry	Samples	n (Co source) (g)	n (Fe source) (g)	η_{10} for OER (mV)	η_{100} for OER (mV)
1	Co-Fe-0.5	0.415	0.636	267	313
2	Co-Fe-1	0.623	0.477	303	364
3	Co-Fe-1.5	0.747	0.382	251	322
4	Co-Fe-1.75	0.913	0.255	294	364
5	Co-Fe-2	0.830	0.318	257	304
6	Co-Fe-2.25	0.862	0.294	276	344
7	Co-Fe-2.5	0.890	0.273	284	365
8	Co-Fe-3	0.934	0.239	274	372
9	Co-Fe-4	0.996	0.191	333	401
10	CP	/	/	480	/

Table S2 The OER performances of nonnoble-based electrocatalysts that reported recently.

	Overpotential (mV)	Tafel (mV dec^{-1})	Current density (mA cm^{-2})	Res.
Co_2P/FeP	257	39.6	10	This work
FeP	416	73.2	10	This work
Co_2P	400	68.2	10	This work
$CoFe_2O_4$	309	67.4	10	[8]
Co_3O_4	278	41	10	[9]
$Co_{3-x}Pd_xO_4$	370	60	10	[10]
FeP_4/CoP/C	258	41	10	[11]
Fe-Ni-Pi-5-SHP	263	44	10	[12]
Co_3Cu-Ni_2MNs	288	87	10	[13]
Ni_3N@2M-MoS_2	327	38.9	10	[14]
MoS_2/NiS_2	381	92	10	[15]
FeP	470	137	10	[16]
CoP	340	114	10	[16]
Fe_2P/NiCoP	272	92.1	10	[17]
Fe_2P@FeN_3P_1-NC	320	46.4	10	[18]
FeP/CoP	266	60.86	10	[19]
Fe_2O_3/FeP	264	47	10	[20]
FeP@Au	320	56.8	10	[21]
CoP	345	47	10	[21]
Ni–P	344	49	10	[21]
CoNiFeP@C NPs	260	65.5	10	[22]
NiFeP/CoP	274	70	10	[23]

Table S3 D-band center of Co_2P, FeP, and Co_2P/FeP

	Co_2P	**FeP**	**Co_2P/FeP**
d-band-center-up	-1.67	-2.072	-1.532
d-band-center-down	-0.924	-0.484	-0.958
d-band-center	-1.297	-1.278	-1.245

References

1 G. Kresse and J. Furthmüller, *Phys. Rev. B*, 1996, **54**, 11169–11186.
2 J. P. Perdew, K. Burke and M. Ernzerhof, *Phys Rev Lett.*, 1996, **77**, 3865.
3 B. Hammer, L. B. Hansen and J. K. Nørskov, *Phys. Rev. B*, 1999, **59**, 7413–7421.
4 S. Grimme, *J. Comput. Chem.*, 2006, **27**, 1787–1799.
5 E. Skúlason, V. Tripkovic, M. E. Björketun, S. Gudmundsdóttir, G. Karlberg, J. Rossmeisl, T. Bligaard, H. Jónsson and J. K. Nørskov, *J. Phys. Chem. C*, 2010, **114**, 18182–18197.
6 G. Gao, A. P. O'Mullane and A. Du, *ACS Catal.*, 2017, **7**, 494–500.
7 S. L. Zhang, B. Y. Guan, X. F. Lu, S. Xi, Y. Du and X. W. (David) Lou, *Adv. Mater.*, 2020, **32**, 2002235.
8 Y. Wang, J. Jia, X. Zhao, W. Hu, H. Li, X. Bai, J. Huang, J. Zhang, J. Li, X. Tang, Y. Peng, J. Huang and C. Xu, *ACS Catal.*, 2024, **14**, 2313–2323.
9 N. Wang, P. Ou, R. K. Miao, Y. Chang, Z. Wang, S.-F. Hung, J. Abed, A. Ozden, H.-Y. Chen, H.-L. Wu, J. E. Huang, D. Zhou, W. Ni, L. Fan, Y. Yan, T. Peng, D. Sinton, Y. Liu, H. Liang and E. H. Sargent, *J. Am. Chem. Soc.*, 2023, **145**, 7829–7836.
10 N. Wang, P. Ou, S. Hung, J. E. Huang, A. Ozden, J. Abed, I. Grigioni, C. Chen, R. K. Miao, Y. Yan, J. Zhang, Z. Wang, R. Dorakhan, A. Badreldin, A. Abdel-Wahab, D. Sinton, Y. Liu, H. Liang and E. H. Sargent, *Adv. Mater.*, 2023, **35**, 2210057.
11 P. Zhao, C. Peng, Y. Luo, L. Cheng, Z. Li and Z. Jiao, *Chem. Eng. J.*, 2024, **483**, 149121.
12 C. Xuan, T. Shen and B. Hou, *Chem. Eng. J.*, 2024, **479**, 147723.
13 P. Dong, Y. Gu, G. Wen, R. Luo, S. Bao, J. Ma and J. Lei, *Small*, 2023, **19**, 2301473.
14 T. Wu, E. Song, S. Zhang, M. Luo, C. Zhao, W. Zhao, J. Liu and F. Huang, *Adv. Mater.*, 2022, **34**, 2108505.
15 Z. Yin, X. Liu, S. Chen, H. Xie, L. Gao, A. Liu, T. Ma and Y. Li, *Mater. Today Nano*, 2022, **17**, 100156.
16 S. Hou, A. Zhang, Q. Zhou, Y. Wen, S. Zhang, L. Su, X. Huang, T. Wang, K. Rui, C. Wang, H. Liu, Z. Lu and P. He, *Nano Res.*, 2023, **16**, 6601–6607.
17 L. Jin, H. Xu, K. Wang, L. Yang, Y. Liu, X. Qian, G. He and H. Chen, *Appl. Surf. Sci.*, 2024, **657**, 159777.
18 E. Zhu, C. Shi, J. Yu, H. Jin, L. Zhou, X. Yang and M. Xu, *Appl. Catal. B Environ. Energy*, 2024, **347**, 123796.
19 X. Lei, J. Qing, L. Weng, S. Li, R. Peng, W. Wang and J. Wang, *New J. Chem.*, 2022, **46**, 15351–15357.
20 I. Ahmad, J. Ahmed, S. Batool, M. N. Zafar, A. Hanif, Zahidullah, M. F. Nazar, A. Ul-Hamid, U. Jabeen, A. Dahshan, M. Idrees and S. A. Shehzadi, *J. Alloys Compd.*, 2022, **894**, 162409.
21 J. Masud, S. Umapathi, N. Ashokaan and M. Nath, *J. Mater. Chem. A*, 2016, **4**, 9750–9754.
22 C. Zhang, Z. Xing, Y. Peng, H. Zhou, L. Zhang and Z.-H. Lu, *Fuel*, 2024, **365**,

131181.
23 G.-L. Li, Y.-Y. Miao, F. Deng, S. Wang, R.-X. Wang, W.-H. Lu and R.-L. Chen, *J. Colloid Interface Sci.*, 2024, **667**, 543–552.